Abdominal Imaging

Published online: 8 August 2005

Abdom Imaging (2005) 30:524–534
DOI: 10.1007/s00261-004-0289-x

UPDATE

Gastrointestinal tract perforation: CT diagnosis of presence, site, and cause

A. Furukawa,[1] M. Sakoda,[1] M. Yamasaki,[1] N. Kono,[1] T. Tanaka,[1] N. Nitta,[1] S. Kanasaki,[2] K. Imoto,[3] M. Takahashi,[1] K. Murata,[1] T. Sakamoto,[3] T. Tani[4]

[1]Department of Radiology, Shiga University of Medical Science, Seta Tsukinowa-cho Otsu, Shiga 520-2192, Japan
[2]Department of Radiology, Kouseikai Takeda Hospital, 841-5 Nishimotoin Highashi-iru Shiokoj-dori Shimogyo-ku, Kyoto, 600-8558, Japan
[3]Department of Radiology, Koga City Hospital, 3-39 Kafuka Minakuchi-cho Kohka, Shiga 528-0014, Japan
[4]Department of Surgery, Shiga University of Medical Science, Seta Tsukinowa-cho Otsu, Shiga 520-2192, Japan

Abstract

Gastrointestinal tract perforation is an emergent condition that requires prompt surgery. Diagnosis largely depends on imaging examinations, and correct diagnosis of the presence, level, and cause of perforation is essential for appropriate management and surgical planning. Plain radiography remains the first imaging study and may be followed by intraluminal contrast examination; however, the high clinical efficacy of computed tomographic examination in this field has been well recognized. The advent of spiral and multidetector-row computed tomographic scanners has enabled examination of the entire abdomen in a single breath-hold by using thin-slice sections that allow precise assessment of pathology in the alimentary tract. Extraluminal air that is too small to be detected by conventional radiography can be demonstrated by computed tomography. Indirect findings of bowel perforation such as phlegmon, abscess, peritoneal fluid, or an extraluminal foreign body can also be demonstrated. Gastrointestinal mural pathology and associated adjacent inflammation are precisely assessed with thin-section images and multiplanar reformations that aid in the assessment of the site and cause of perforation.

Key words: Perforation—Gastrointestinal tract—Alimentary tract—CT

Gastrointestinal (GI) tract perforation is an emergent condition that usually requires prompt surgery. It can result from different spontaneous, traumatic, or iatrogenic causes and has variable clinical presentations, particularly in the early clinical course. Diagnosis largely depends on imaging examinations, and correct diagnosis of the presence, level, and cause of perforation is important for appropriate patient management and surgical planning. The diagnosis of GI tract perforation is generally based on identification of extraluminal leakage and consequent inflammatory reaction around the perforated site. Plain radiography remains the first imaging study and may be followed by luminal contrast examination; however, the high clinical efficacy of computed tomographic (CT) examination in this field has been well recognized [1–19]. The advent of spiral and multidetector-row CT scanners has enabled examination of the entire abdomen in a single breath-hold by using thin-slice that allow precise assessment of pathology in the alimentary tract [2]. In this article, the characteristic CT findings indicating the presence, sites, and causes of perforation are described, and CT appearances of GI tract perforation at various levels are demonstrated.

Plain radiography and contrast examination

Plain radiography has been the first modality of choice in patients with suspected GI tract perforation. The hallmark of alimentary tract perforation on plain films is the presence of air outside the gut lumen. The extraluminal air may be in the free peritoneal cavity, retroperitoneal spaces, mesentery, or ligaments of organs. Pneumomediastinum and/or subcutaneous emphysema may also be seen. In addition to upright and supine abdominal radiographic images, upright chest films and/or left lateral decubitus abdominal films should be included for the

Correspondence to: A. Furukawa; *email:* akira@belle.shiga-med.ac.jp

Fig. 1. Contrast enema study in a patient with spontaneous sigmoid colonic perforation. Extravasation of luminal contrast medium is demonstrated.

Fig. 2. Barium enema study in a patent with Crohn disease. Extravasation of barium demonstrates sinus tracts in the descending colon.

assessment of GI tract perforation [20]. However, extraluminal air may not be demonstrable if the perforation is very small, self-sealed, or well contained by adjacent organs. The reported sensitivity in the detection of extraluminal air on plain radiography is 50% to 70% [1, 21–23]. When perforation of the gut is not demonstrable by plain radiography and a more precise assessment regarding the specific site and cause of perforation is needed, a contrast examination may be indicated (Figs. 1, 2). Water-soluble iodinated contrast material is administrated orally or transrectally depending on the suspected site of perforation. Although initial use of barium in patients with a known or suspected perforation is contraindicated, it may be used when the water-soluble iodinated contrast material fails to demonstrate extraluminal leakage [23, 24].

Computed tomography

CT is an easy and very sensitive imaging modality in diagnosing GI tract perforation. It can display intra- and extraperitoneal air that is too small to be demonstrated on plain radiography [3–5, 23]. In addition to the presence, site, and cause of perforation and associated complications such as phlegmon, abscess and peritonitis can be demonstrated in most cases. The entire abdomen including the level above the diaphragm to the bottom of the pelvis should be scanned by using 1- to 2.5-mm collimation when a multidetector row CT scanner is used. Contiguous axial images 5 to 7 mm thick are obtained and thinner sections or multiplanar reconstruction may be applied when necessary. Oral or rectal contrast administration before the examination is recommended, although extraluminal leakage of contrast is not a frequent CT finding in patients with alimentary tract perforation [1]. Use of intravenous contrast injection (300 to 370 mg I/mL; 100 to 150 mL at a rate of 2 to 3 mL/s) is necessary and will aid in the assessment of the site and cause of perforation (Fig. 3). Diagnosis of alimentary tract perforation is based on direct findings of extraluminal air or luminal contrast material and discontinuation of the GI wall and on indirect findings of abscess and an inflammatory mass or phlegmon related to the bowel with or without associated an enterolith or foreign body (Figs. 3–10) [1, 5, 6]. To enhance sensitivity to detect extraluminal air, CT images should also be assessed in the wide window setting that distinguishes air from fat densities (Fig. 11) [1, 25]. Particular attention should be paid to the anterior peritoneal surfaces of the liver and midabdomen and among the peritoneal folds so as not to overlook a small amount of extraluminal air (Figs. 12, 13) [1, 25]. The site of perforation can be assessed by CT findings of (a) discontinuation of the GI wall, (b) the site of luminal contrast medium leakage, (c) the level of bo-

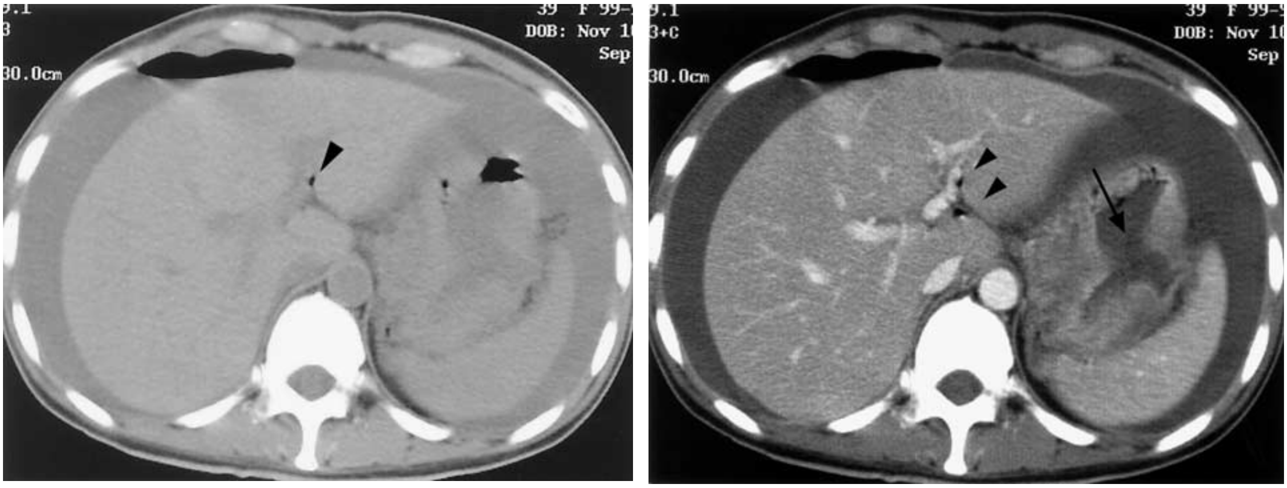

Fig. 3. Unenhanced (**Left**) and contrast-enhanced (**Right**) abdominal CT images of a patient with a perforated gastric ulcer. A large quantity of peritoneal fluid and free air anterior to the liver surface are demonstrated. A small amount of air in the intrahepatic fissure for the ligamentum teres can also be seen (*arrowheads*). A deep ulcer is clearly demonstrated on the greater curvature of the stomach on contrast-enhanced CT (*arrow*).

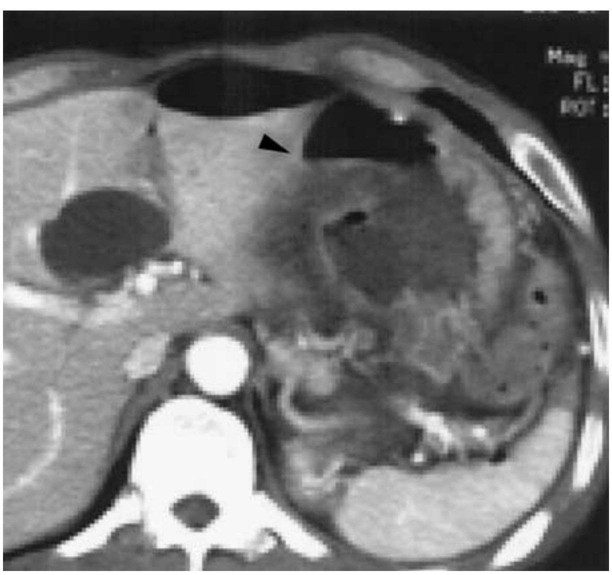

Fig. 4. Contrast-enhanced abdominal CT image of a patient with a perforated gastric peptic ulcer. Discontinuation of the gastric wall on the lesser curvature (arrowhead) indicates the perforated gastric ulcer.

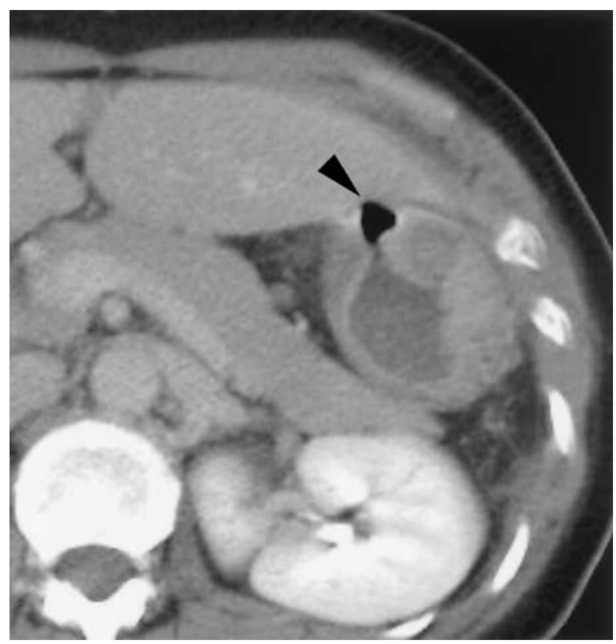

Fig. 5. Contrast-enhanced abdominal CT image of a patient with perforated gastric peptic ulcer disease. Discontinuation of the gastric wall is caused by a deep ulcer (*arrowhead*) associated with surrounding mural thickening.

wel obstruction, and (d) abrupt GI wall thickening with or without an associated phlegmon, inflammatory mass, or abscess (Figs. 3–10, 14, 15) [5]. The site of perforation can also be assessed by the amount and location of extraluminal air on CT images. A large amount of intraperitoneal air usually indicates gastroduodenal perforation, except for bowel perforation which is caused by obstruction or an endoscopic procedure. Air in the lesser sac is commonly due to posterior perforation of the stomach (Fig. 16) or duodenum [20, 26] or, less commonly, from rupture of the lower esophagus [27, 28] or transverse colon [20]. Free air confined in the intrahepatic fissure of the ligamentum teres can be seen in the perforation of the duodenal bulb (Fig. 17) or stomach [29, 30]. Air trapped in the mesenteric folds is found in perforation of the colon and small bowel but is seldom seen in gastric perforation. A pneumoretroperitoneum is caused by perforation of any site where the alimentary

Fig. 6. Contrast-enhanced pelvic CT image of a patient with iatrogenic rectal perforation. Discontinuation of the rectal wall is identified on the left side (*arrowhead*). Inflammatory change in the perirectal fat tissue and a small amount of ascites are displayed.

Fig. 7. Contrast-enhanced pelvic CT image of ileal perforation in a patient with Crohn disease. An abscess in the right abdominal wall indicates perforation (*arrowhead*).

tract is extraperitoneal; normally these sites are the duodenum (descending and horizontal segments), ascending and descending colon, and rectum (Figs. 6, 9) [20]. Perforation of the sigmoid diverticula also causes a pneumoretroperitoneum because three-fourths of the diverticulum is located in the extraperitoneum (Figs. 18,

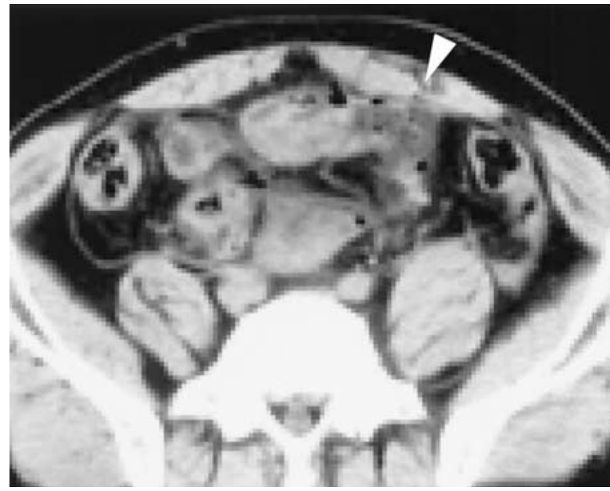

Fig. 8. Unenhanced pelvic CT image of an ileal perforation caused by a blunt abdominal trauma. Air bubbles and hazy density in the fat issue are observed around the perforated ileal loop (*arrowhead*).

Fig. 9. Duodenal perforation caused by migration of a metallic biliary stent. Migration of the stent and pneumoretroperitoneum in the anterior and posterior pararenal spaces are visible.

19) [31–33]. Gas in the retroperitoneum dose not spread freely as in the peritoneal space. Specifically, when the amount is small, it tends to remain regional with respect to the boundaries of the retroperitoneal compartment in which it arises [20, 34, 35]. In general, extraperitoneal gas that originates in the pelvis commonly spreads bilaterally into the anterior and/or posterior pararenal spaces, whereas gas that originates above the pelvic brim tends to remain unilateral and does not cross the midline. Therefore, gas in the right anterior pararenal space indicates duodenal or ascending colon perforations, whereas gas in the left anterior pararenal space indicates descending or sigmoid colon perforations. Bilateral

Fig. 10. Ileal perforation caused by a fish bone. Ileal wall thickening, an abscess in the abdominal wall adjacent to it, and a fish bone (*arrowhead*) in the abscess are demonstrated.

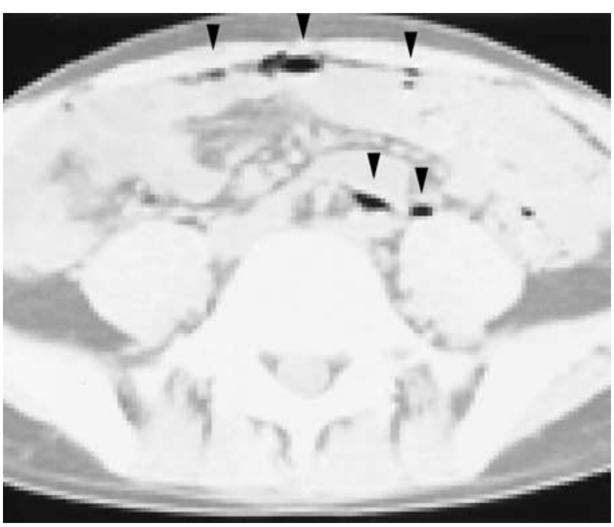

Fig. 11. Small amounts of air at the anterior abdominal surface and in the retroperitoneum (*arrowheads*). The presence of air is more confidently identified on a CT image with a wide window setting than with a conventional window setting.

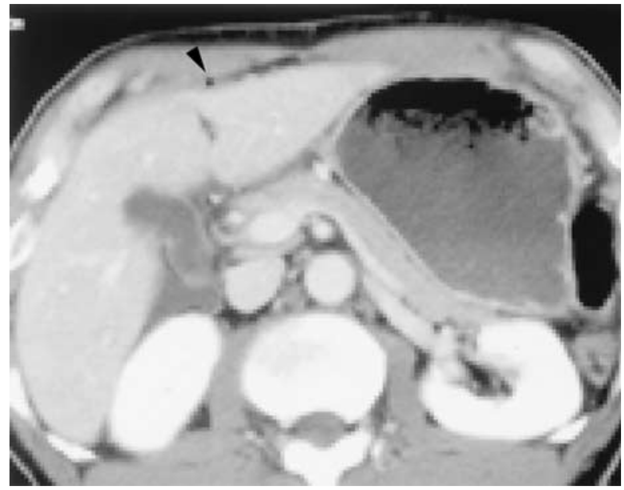

Fig. 12. Contrast-enhanced CT image in a patient with duodenal perforation. An air bubble is seen at the anterior peritoneal surface of the liver (*arrowhead*).

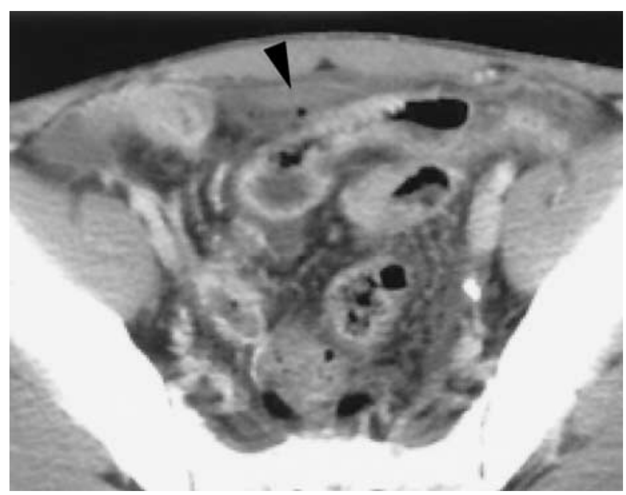

Fig. 13. Contrast-enhanced CT image of an ileal perforation in a patient with Crohn disease. An air bubble is seen adjacent to the perforated ileal loop (*arrowhead*).

pneumoretroperitoneum is caused by rectal perforation [31]. Although air in the peritoneal space can reach the retroperitoneum and vice versa [34], intraperitoneal and extraperitoneal air should suggest an extraperitoneal structure as the source [31]. It should be noted that pneumoperitoneum and pneumoretroperitoneum occur without GI tract perforation [20, 35]. Pneumoperitoneum may be seen as a consequence of gastric distention, diverticulosis, pneumatosis cystoides intestinalis, or scleroderma. Intraperitoneal air may also arise from the thorax or female genital tract [36–38]. Pneumoretroperitoneum can be caused by air from pneumomediastinum.

Level and cause of perforation

Gastroduodenal perforations

Peptic ulcers are the main cause of gastroduodenal perforation, followed by necrotic or ulcerated malignancies. Recently, however, the number has been decreasing because of improvements in procedures for earlier diag-

Fig. 14. Contrast-enhanced CT image in a patient with gastric perforation. Prominent wall thickening is seen at the pyloric antrum (*arrow*).

Fig. 16. Contrast-enhanced CT image in a patient with gastric perforation. Air in the lesser sac is visible (*arrow*). Large amounts of ascites and free air in the anterior peritoneal surface of the liver are demonstrated.

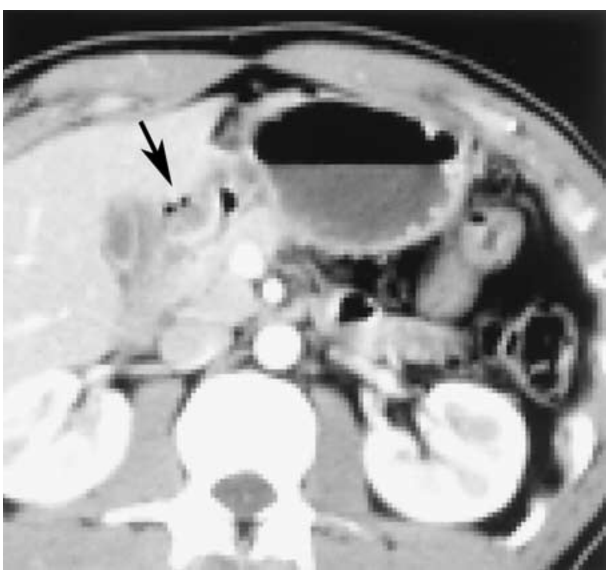

Fig. 15. Contrast-enhanced CT image in a patient with duodenal perforation. Mural thickening of the duodenal bulb and adjacent air bubbles are visible (*arrow*).

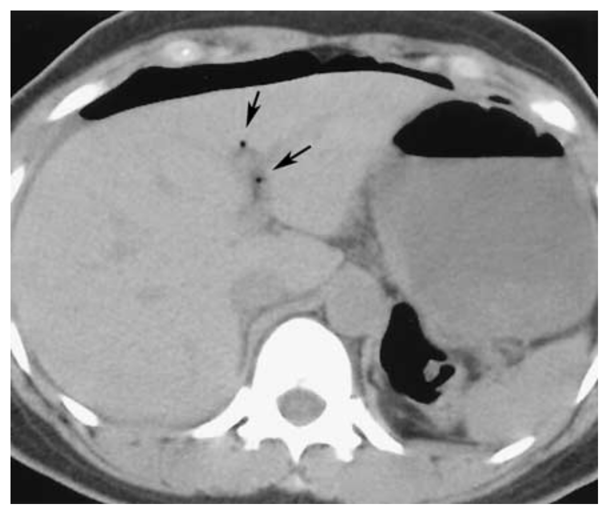

Fig. 17. Contrast-enhanced CT image of duodenal bulb perforation. Air in the intrahepatic fissure for the ligamentum teres is visible (*arrows*). Peritoneal fluid and free air in the anterior peritoneal surface of the liver are demonstrated.

nosis and patient management. Conversely, iatrogenic and traumatic injuries have increased as causes of gastroduodenal perforation [23]. The most common and consistent CT findings of gastroduodenal perforation are extraluminal air and leakage of luminal contrast. Extraluminal air is usually large in amount and it is frequently seen around the liver and stomach [7]. Air in the lesser sac and the intrahepatic fissure of the ligamentum teres is characteristic of gastroduodenal perforation as mentioned previously (Figs. 16, 17) [20, 26, 29, 30]. Sites of perforation are frequently assessed by CT findings of ulceration or focal interruption of the gastroduodenal wall and abrupt wall thickening associated with adjacent increased fat density (Figs. 3–5, 14, 15). Gastroduodenal perforation from traumatic injuries occurs predominantly in the descending and horizontal segments of the duodenum, mostly by blunt trauma in children and by penetrating trauma in adults, and cause pneumoretroperitoneum in the anterior pararenal space [8]. CT is helpful in distinguishing a duodenal hematoma from a perforation [9, 10].

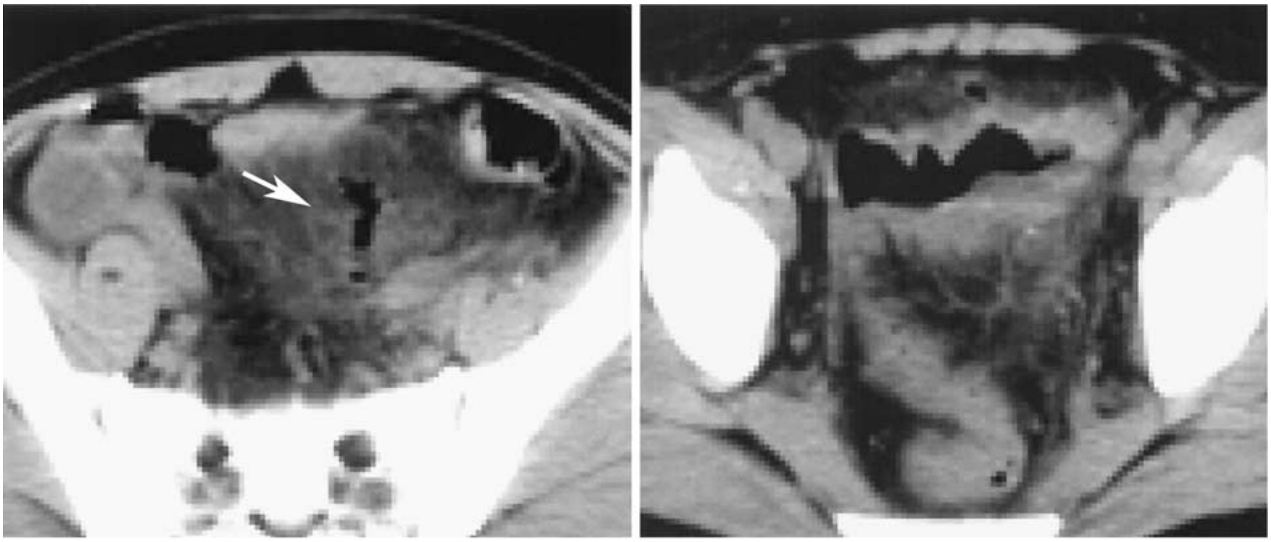

Fig. 18. CT images of perforated sigmoid colonic diverticulitis (**Left** cephalad to **Right**). Prominent mural thickening of the sigmoid colon and hazy density of the surrounding fat tissue are observed. Extraluminal air adjacent to the sigoid colon (pneumoretroperitoneum) is seen (*arrow*).

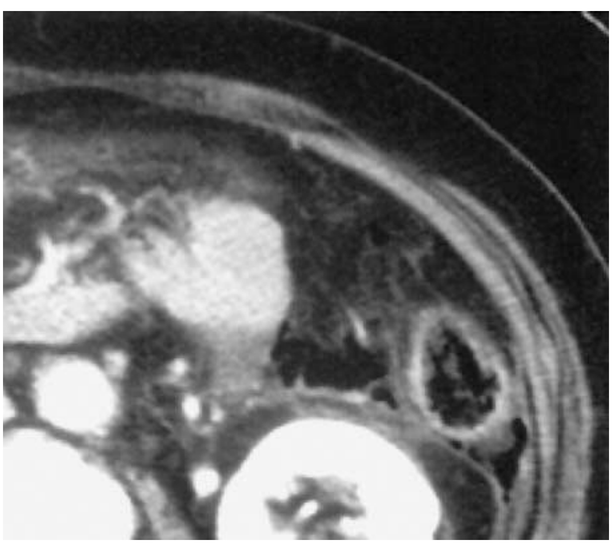

Fig. 19. CT image at the level of the left kidney in a patient with a rupture of the sigmoid colon. Pneumoretroperitoneum is observed in the anterior pararenal space.

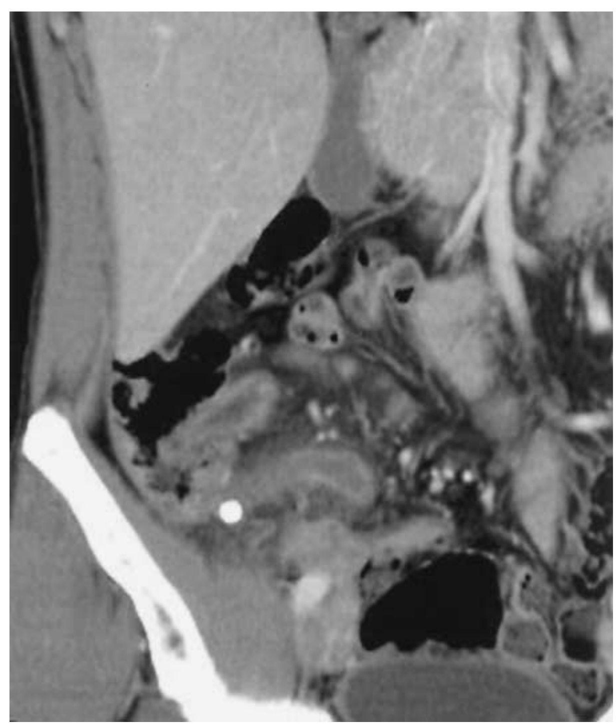

Fig. 20. CT image of acute appendicitis without perforation. The dilated appendix is associated with an appendicolith and surrounding inflammatory change.

Small bowel perforations

The incidence of small bowel perforation is low but can develop from a variety of causes including ischemic or bacterial enteritis, Crohn disease (Figs. 7, 13), diverticulitis, ingested foreign bodies (Fig. 10), bowel obstruction, volvulus, and intussusception [23, 39]. Abdominal trauma (Fig. 8), iatrogenic injury, and postoperative perforation or anastomotic leakage also can cause small bowel perforation [23]. In contrast to gastroduodenal perforation, the amount of extraluminal air in small bowel perforation is small or absent in most cases, and extraluminal air is detected in only approximately 50% of cases even with CT examination [11]. A small amount of gas trapped in the mesenteric folds and indirect findings indicating a perforation should be carefully evaluated

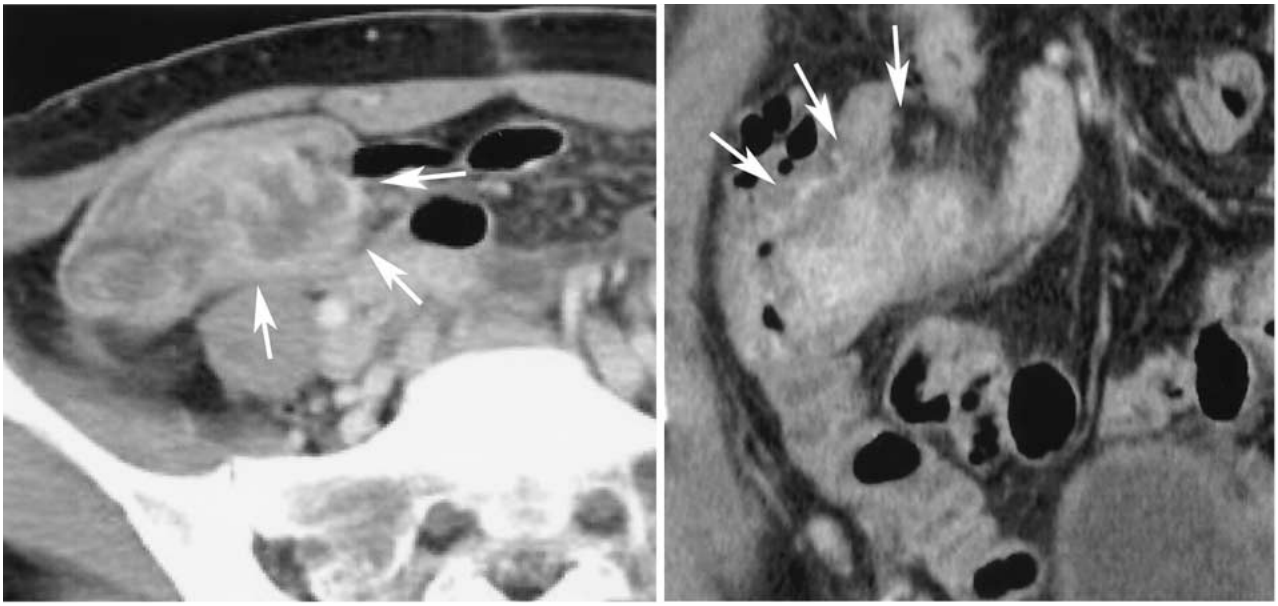

Fig. 21. Contrast-enhanced CT image of a perforated appendicitis in (**Left**) axial and (**Right**) coronal sections. An inflammatory mass is displayed adjacent to the cecum (*arrows*). The proximal site of the appendix is not identifiable.

with CT [11]. When CT findings are nondiagnostic and obvious clinical signs of perforation are absent, close monitoring with repeated CT examination may be indicated. Postoperative perforation or anastomotic leakage usually occurs within the first week after surgery. Because extraluminal air in this period is present in every patient, it cannot be a hallmark of the presence of intestinal perforation or leakage. Perforation or leakage should be suspected with persistent or progressively increasing free air and must be confirmed by contrast examination with water-soluble iodinated contrast material [11, 23, 40].

Appendiceal perforations

CT has been established as the imaging study of choice for the diagnosis of acute appendicitis, with sensitivities and specificities ranging from 94% to 98% based on findings of a thickened appendix with some degree of adjacent inflammation (Fig. 20) [12–17]. Surgery is indicated for most patients with acute appendicitis, but it tends to be avoided once perforation has occurred because of the relatively high rates (12% to 30%) of perioperative complications [12, 17, 41]. Therefore, distinguishing nonperforated from perforated appendicitis is clinically important but not always simple because rupture of the appendix can be a localized process and may not show typical clinical presentation. In addition, the amount of extraluminal air is usually small or absent, usually no more than 1 or 2 mL, in perforated appendicitis because acute appendicitis is typically initiated by luminal obstruction [20]. High performance of CT diagnosis for perforated appendicitis has recently been reported with combined findings of extraluminal air, extraluminal appendicolith, abscess, phlegmon, and a defect in enhancing the appendiceal wall with a sensi-

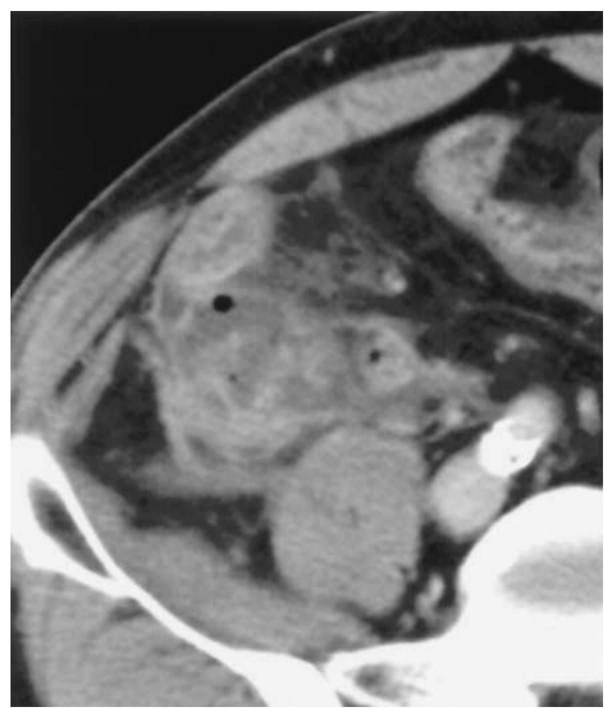

Fig. 22. Contrast-enhanced CT image of perforated acute appendicitis. Phlegmon associated with gas bubbles is demonstrated at the periappendiceal region. The appendix itself is not visible.

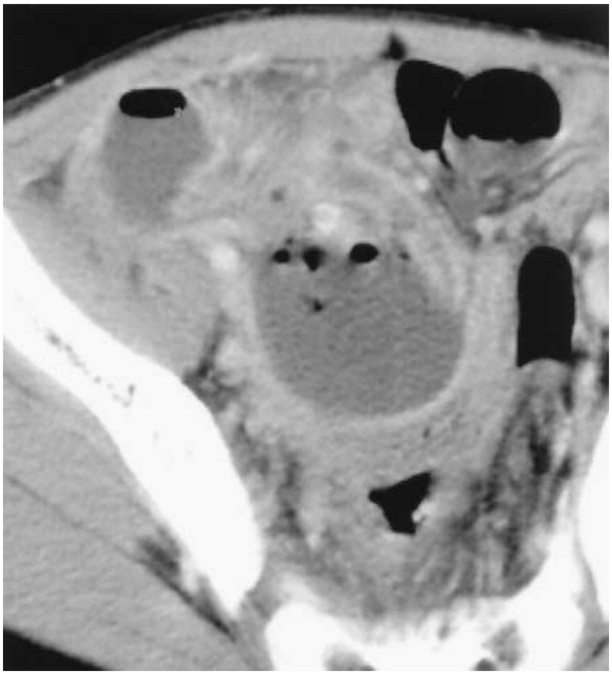

Fig. 23. Contrast-enhanced CT image of perforated appendicitis. A large abscess containing gas bubbles is observed at the periappendiceal region. The appendix itself is not identified.

tivity of 94.9% and a specificity of 94.5% (Figs. 21–23) [12, 17]. CT should be indicated for patients with known or suspected acute appendicitis to assess severity and exclude other conditions.

Large bowel perforations

Malignant neoplasm (Fig. 24), diverticulitis (Fig. 18), and spontaneous perforation (Fig. 25) are major causes of large bowel perforation, followed by trauma, ischemia, and different inflammatory lesions and iatrogenic causes [18, 19, 23]. Perforations from malignant neoplasm, spontaneous perforation, diverticulitis, blunt trauma, and ischemia tend to occur in the left colon, whereas those from inflammatory lesions and penetrating trauma are frequently observed in the right colon [23, 42]. The cecum is predisposed to perforate when the intraluminal pressure of the colon is increased, as in cases of bowel obstruction and toxic megacolon. The rectum and sigmoid colon are the predominant sites of iatrogenic injuries [23]. Perforations of the large bowel may occur in intraperitoneal or retroperitoneal spaces, depending on the portion that perforates. A large amount of free air is seen when perforation complicates bowel obstruction or an endoscopic procedure [23, 43]. In cases of perforated diverticulitis, the amount of extraluminal air is usually small and perforation usually occurs into the retroperitoneal space because most diverticula of the colon are located in the retroperitoneum between the taenia mesocolica and libera and between the taenia mesocolica and omentalis [31–33]. The amount of extraluminal air is usually small in cases of perforated colorectal neoplasm without bowel obstruction. Barium or water-soluble contrast enema may be indicated when extraluminal air is not visible on plain radiography; however, the sensitivity of contrast enema study is not always high and it should be used prudently in cases

Fig. 24. Contrast-enhanced CT image of sigmoid colon perforation caused by cancer. Mural thickening at the sigmoid colon indicates the presence of cancer (arrow). Extraluminal air (*arrowhead*) and increased fat density in the pelvis are visible.

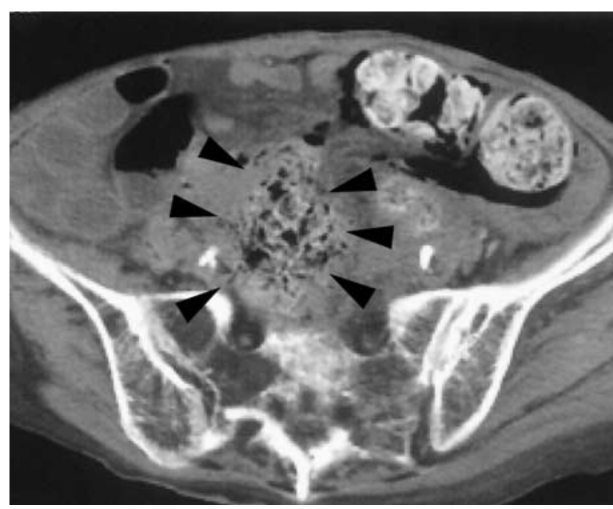

Fig. 25. Contrast-enhanced CT image of spontaneous perforation of the sigmoid colon (the same patient as shown in Fig. 1). Perforated extraluminal feces display a unique appearance of a mass with mottled radiolucence in the pelvis (arrowheads).

where the bowel wall is already weak and friable due to inflammatory, ischemic, or neoplastic changes [23]. The presence of an underlying colonic lesion and associated extraluminal air and surrounding phlegmon and/or abscess should be carefully examined with CT (Fig. 24) [44]. In cases of spontaneous perforation of the colon, which is occasionally seen at the sigmoid colon, perforated extraluminal feces demonstrate a unique appearance of a mass with mottled radiolucence in the pelvis (Fig. 25) [18, 44].

Conclusion

Correct diagnosis of the presence, level, and cause of perforation is essential for appropriate management and surgical planning in patients with GI perforation. CT has high performance in diagnosing the presence of perforation by demonstrating extraluminal air too small to be detected by conventional radiography. Indirect findings of bowel perforation such as phlegmon, abscess, peritoneal fluid, or extraluminal foreign body can also be demonstrated. With a spiral or multidetector row CT scanner, GI mural pathology and adjacent inflammation are precisely assessed with thin-section images and multiplanar reformations that aid in the assessment of the site and cause of perforation.

References

1. Maniatis V, Chryssikopoulos H, Roussakis A, et al. (2000) Perforation of the alimentary tract: evaluation with computed tomography. Abdom Imaging 25:373–379
2. Ongolo-Zogo P, Borson O, Garcia P, et al. (1999) Acute gastro-intestinal peptic ulcer perforation: contrast-enhanced and thin-section spiral CT findings in 10 patients. Abdom Imaging 24:329–332
3. Jeffrey RB, Federle MP, Wall S (1983) Value of computed tomography in detecting occult gastrointestinal perforation. J Comput Assist Tomogr 7:825–827
4. Stapakis JC, Thickman D (1992) Diagnosis of pneumoperitoneum: abdominal CT vs. upright chest film. J Comput Assist Tomogr 16:713–716
5. Chen CH, Huang HS, Yang CC, et al. (2001) The features of perforated peptic ulcers in conventional computed tomography. Hepatogastroenterology 48:1393–1396
6. Lee H, Vibhakar SD, Bellon EM (1983) Gastrointestinal perforation: early diagnosis by computed tomography. J Comput Assist Tomogr 7:226–229
7. Fultz PJ, Skucas J, Weiss CL (1992) CT in upper gastrointestinal perforation secondary to peptic ulcer disease. Gastrointest Radiol 17:5–8
8. Glazer GM, Buy JN, Moss AA, et al. (1981) CT detection of duodenal perforation. AJR 137:333–336
9. Hofer GA, Cohen AJ (1989) CT signs of duodenal perforation secondary to blunt abdominal trauma. J Comput Assist Tomogr 13:430–432
10. Shilyansky J, Pearl RF, Kreller M, et al. (1997) Diagnosis and management of duodenal injury in children. J Pediatr Surg 32:880–886
11. Grassi R, Pinto A, Rossi G, et al. (1998) Conventional plain film radiology ultrasonography and CT in jejuno-ileal perforation. Acta Radiol 39:52–56
12. Horrow MM, White DS, Horrow DO, JC (2003) Differentiation of perforated from nonperforated appendicitis at CT. Radiology 227:46–51
13. Rao PM, Rhea JT, Novelline RA (1997) Sensitivity and specificity of the individual CT signs of appendicitis: experience with 200 helical appendiceal CT examinations. J Comput Assist Tomogr 21:686–692
14. Balthazar EJ, Megibow AJ, Siegel SE, et al. (1991) Appendicitis: prospective evaluation with high-resolution CT. Radiology 180:21–24
15. Rao PM, Rhea JT, Novelline RA (1997) Helical CT technique for the diagnosis of appendicitis: prospective evaluation of a focused appendix CT examination. Radiology 202:139–144
16. Wijetunga R, Tan BT, Rouse JC, et al. (2001) Diagnostic accuracy of focused appendiceal CT in clinically equivocal cases of acute appendicitis. Radiology 221:7474–753
17. Oliak D, Sinow R, French S, et al. (1999) Computed tomography scanning for the diagnosis of perforated appendicitis. Am Surg 65:959–964
18. Saeki M (1988) Computed tomographic analysis of colonic perforation; "dirty mass" a new computed tomographic finding. Emerg Radiol 5:140–145
19. Hulnick DH, Megibow AJ, Balthazar EJ, et al. (1987) Perforated colorectal neoplasms: correlation of clinical, contrast enema, and CT examinations. Radiology 164:611–615
20. Shaffer HA (1992) Perforation and obstruction of the gastrointestinal tract. Assessment by conventional radiology. Radiol Clin North Am 30:405–426
21. Cho KC, Baker SR, Cho KC, Baker SRExtraluminal air. Diagnosis and significance. Radiol Clin North Am 1994;32;829–844
22. Rice RP, Thompson VM, Gegaudas RK (1982) The diagnosis and significance of extraluminal gas in the abdomen. Radiol Clin North Am 20:819–837
23. Ghahremani GG, Ghahremani GG (1993) Radiologic evaluation of suspected gastrointestinal perforations. Radiol Clin North Am 1993;31;1219–1234
24. Foley MJ, Ghahremani GG, Rogers LF (1982) Reappraisal of contrast media used to detect upper gastrointestinal perforations. Comparison of water-soluble media with barium sulfate. Radiology 144:231–237
25. Cho KC, Baker SR (1994) Extraluminal air. Diagnosis and significance. Radiol Clin North Am 32:829–844
26. Cimmino CV, Sholes DK Jr (1952) Gas in the lessor sac in perforated peptic ulcer. AJR 68;19–21
27. Han SY, Tishler JM (1984) Perforation of the abdominal segment of the esophagus. AJR 143:751–754
28. Healy ME, Mindelzun RE (1984) Lesser sac pneumoperitoneum secondary to perforation of the intraabdominal esophagus. AJR 142:325–326
29. Cho (2000) Manifestations of intraperitoneal air. In: Meyers MA, ed. *Dynamic radiology of the abdomen*. New York: Springer-Verlag, pp 309–331
30. Cho KC, Baker SR (1781) Air in the fissure for the ligamentum teres: new sign of intraperitoneal air on plain radiographs. Radiology 91:489–492
31. Meyers MA (2000) The extraperitoneal spaces: normal and pathologic anatomy. In: Meyers MA, ed. *Dynamic radiology of the abdomen*. New York: Springer-Verlag, pp 333–492
32. Meyers MA, Volberg F, Katzen B, et al. (1973) Haustral anatomy and pathology: a new look. I. Roentgen identification of normal patterns and relationships. Radiology 108:497–504
33. Meyers MA, Volberg F, Katzen B, et al. (1973) Haustral anatomy and pathology: a new look. II. Roentgen identification of normal patterns and relationships. Radiology 108:505–512
34. Stahl JD, Goldman SM, Minkin SD, et al. (1977) Perforated duodenal ulcer and pneumomediastinum. Radiology 124:23–25
35. Roh JJ, Thompson JS, Harned RK, et al. (1983) Value of pneumoperitoneum in the diagnosis of visceral perforation. Am J Surg 146:830–833
36. Felson B, Wiot JF (1973) Another look at pneumoperitoneum. Semin Roentgenol 8:437–443
37. Miller RE, Becker GJ, Slabaugh RD (1981) Nonsurgical pneumoperitoneum. Gastrointest Radiol 6:73–74
38. Dunn V, Nelson JA (1979) Jejunal diverticulosis and chronic pneumoperitoneum. Gastrointest Radiol 4:165–168

39. Greenstein AJ, Mann D, Heimann T, et al. (1987) Spontaneous free perforation and perforated abscess in 30 patients with Crohn's disease. Ann Surg 205:72–76
40. Ghahremani GG, Gore RM (1989) CT diagnosis of postoperative abdominal complications. Radiol Clin North Am 27:787–804
41. Hele DA, Molly M, Pearl RH, et al. (1997) Appendectomy: a contemporary appraisal. Ann Surg 225:252–261
42. Bugis SP, Blair NP, Letwin ER (1992) Management of blunt and penetrating colon injuries. Am J Surg 163:547–550
43. Meyers MA, Ghahremani GG (1975) Complications of fiberoptic endoscopy. II. Colonoscopy. Radiology 115:301–307
44. Miki T, Ogata S, Uto M, et al. (2004) Multidetector-row CT findings of colonic perforation: direct visualization of ruptured colonic wall. Abdom Imaging 29:659–662